



EFFECTS OF NONLINEARITY IN TROPICAL SOILS ON THE STRUCTURE PERFORMANCE

S. Montoya-Noguera

⁽¹⁾ Associate Professor, Universidad EAFIT, Department of Civil Engineering, Applied Mechanics Research Group, smontoyan@eafit.edu.co

Abstract

The metropolitan area of the Aburrá Valley (AMVA, by its Spanish acronym) is an earthquake-prone region in Colombia. The alluvial deposits found in this valley present a complex geotechnical behavior. In the center of the valley, along the Medellín River, broad alluvial deposits are found varying between 12 and 42 m in depth. The shear wave velocities (V_s) in the upper 10 m can be as low as 150 m/s. Additionally, according to several cyclic tests, large variability is present in the shear modulus reduction and damping evolution curves. Some data presents less degradation and higher damping at low and intermediate strain levels than common empirical relationships found in the literature. This variability may be related to the degree of sample disturbance, system compliance in triaxial tests or the effect of largely variable state and characteristic parameters.

With the purpose of identifying general aspects of all alluvial deposits in the AMVA region, the microzonation study of 2018 presented the mean soil amplification factors (AFs) as the ratio of spectral accelerations on the surface with respect to the ones at the outcropping rock. These AFs were obtained by Monte Carlo simulations with equivalent linear analysis of 1D wave propagation. Different sources of uncertainty were included such as different input motions, variability in V_s profile, and variability in modulus reduction curves (MRCs), among others. While equivalent-linear analysis is probably the most used procedure in practice, two main limitations are worth mentioning: overestimation of maximum acceleration, and underestimation of high frequency amplification. Additionally, it is incapable of representing the changes in soil stiffness that occur during the earthquake due to strain accumulation or the effects of the structure on the soil.

Generally, the effects of soil nonlinearity and soil-structure interaction are assumed beneficial and thus ignored. However, an accurate evaluation of the expected structural seismic response may improve engineering practice and reduce costs. The aim of this study is to assess the effects of SSI and soil nonlinearity on the structure's performance. For this purpose, the results of several cyclic tests on alluvial soils are used to quantify the effect on the variability of the shear modulus reduction and damping evolution curves. Two sets of MRCs are obtained representing the uncertainty in the various cyclic tests. Then, several finite element computations are performed with a coupled nonlinear model to analyze the effect of input motion and V_s variability. The results show that V_s variability effect on the variability of AF is similar for each input motion, but that it is greatly affected by the MRC used. Finally, a typical reinforced structure is used to combine the effect of SSI with the two sets of MRCs. For all motions tested, when the reduction of the shear modulus is presented at higher strains, the peak accelerations at surface, and the inter-story drift may be twice as large. However, the effect on the settlement of the structure is not clear, as this value may be affected by other soil and motion parameters. The results highlight the importance of accurately assessing the soil behavior and the input motion used, especially when including variability. Combining various sources of uncertainty may reduce the median AFs, which could be highly prejudicial for some sites.

Keywords: nonlinear constitutive models; tropical soils; alluvial deposits; cyclic tests; soil-structure interaction



1. Introduction

In Colombia, the level of seismic risk gets aggravated by the vulnerable population and building stock [1]. The city of Medellín, which is part of the metropolitan area of the Aburrá Valley (AMVA), is one example of significant seismic risk. Compared to other regions in Colombia, it is an intermediate seismic hazard zone. However, more than 60% of the building stock are unreinforced masonry structures, which represent high seismic vulnerability [2]. Recently, Yamin et al. [3] applied a probabilistic procedure to develop a new AMVA seismic microzonation integrating the available information to consider local soil response in the assessment of seismic hazard. While previous microzonations had only considered the average shear-wave velocity in the upper 30m (V_{s30}) to account for site effects, this study performed multiple Monte Carlo simulations including different sources of uncertainty.

Seismic hazard assessment is strongly influenced by nonlinear site effects. However, the limited number of in-situ and laboratory test data, the effects of sample disturbance and the natural heterogeneity of soil deposits are significant sources of uncertainty in nonlinear site-response predictions. Additionally, intensity and frequency content of the input motions and the constitutive soil model used, strongly affect the assessment. Statistical analyses of data to determine geotechnical parameters have been discussed broadly in the literature ([4]–[6], among others). However, most of the available methods focus on point statistics (e.g. mean and standard deviation) and hence ignore the spatially varying pattern of soil properties [7]–[9]. According to several studies (e.g. [10]–[12]), seismic hazard assessment is strongly dependent of the uncertainties in the modulus reduction curves (MRCs) and in shear-wave velocity (V_s) profiles. Rathje et al. [10] quantified the effect of including the uncertainty in both MRC and V_s profiles, as well as the effect of varying the number of input motions used. Their results show that including large amounts of uncertainty in V_s profiles can result in 25% to 50% reductions in the median response spectrum of surface acceleration (SA) and associated amplification factors (AFs) defined as the ratio of spectral accelerations on the surface with respect to the ones at the outcropping rock. Additionally, when both the V_s profile and the MRC uncertainties are included, the median AFs continue to decrease. This median reduction is accompanied by an increase in the standard deviation; however, it is generally insufficient to overcome the decrease in the median values. Rathje et al. [10] performed one-dimensional equivalent linear (EQL) analysis; while Li and Assimaki [11] presented a similar study but using a hysteretic soil model to simulate the large-strain response and used extensive geotechnical data on the variability statistics at 3 downhole array sites and 500 input motions. Similar results were presented highlighting the stronger effect of MRC variability in soft soil profiles and their dependence on the seismic motion intensity. In contrast, the uncertainty in V_s profiles was less sensitive to the motion's intensity. Most importantly, the authors conclude that these results are site and ground-motion specific, thus further research is needed to fully understand the dominant sources of uncertainty in site-response analysis.

The recent study for seismic microzonation in AMVA consisted in a probabilistic assessment of seismic hazard considering local soil response [3]. The region was divided in 17 geotechnical zones assumed homogeneous “in terms of the depth to competent rock, soil stratigraphy, and mechanical and geotechnical properties” [3]. More than one hundred soil profiles and careful revision of geological, geomorphological and geotechnical information was gathered to define these zones. As a result, for each geotechnical zone, the average depth to bedrock and the type of soils in the deposit were given. Concerning the profiles, the mean and standard deviation values for V_s and the unit weight were provided each meter. This information is required to evaluate the fundamental soil vibration period (T_{soil}) of the deposit and to classify the profile according to the site classes of NEHRP [13], which are the same as for the Colombian building code NSR-10 [14]. To include soil nonlinearity, the average and standard deviation of the shear modulus reduction and damping curves with respect to shear strain were also provided. In the center of the valley, along the Medellín River, broad alluvial deposits are found varying between 12 and 42 m in depth. The alluvial deposits present complex geotechnical behavior where V_s in the upper 10 m can be as low as 150 m/s and often V_s inversions are found. Additionally, according to several cyclic tests, large variability is present in the shear modulus degradation, and damping evolution curves. Some data presents less degradation and higher damping at low and intermediate strain levels than common empirical relationships found in the literature. This variability may be related to the degree of sample disturbance, system compliance in triaxial tests or the effect of largely variable state and characteristic parameters.

The results of the site effects including the different sources of uncertainty were presented as mean soil amplification factors (AFs) for each geotechnical zone. Different mean AFs were provided for different intensity levels, measured by the peak horizontal acceleration (PHA) at the outcropping rock, and different values of the soil resonant period (T_{soil}). For example, for the alluvial deposits, mean AFs presented varied from 0.5 for structural periods (T_{st}) about 0.1 s to above 3, for T_{st} about 1 s, when T_{soil} is about 0.7 s and PHA is 0.2 g [3]. These AFs were obtained by Monte Carlo simulations with equivalent linear analysis of 1D wave propagation. While equivalent-linear analysis is probably the most used procedure in practice, two main limitations are worth mentioning: overestimation of maximum acceleration, and underestimation of high frequency amplification. Additionally, these analyses are incapable of



representing the changes in soil stiffness that occur during the earthquake due to strain accumulation or softening due to pore-water pressure generation.

Generally, the soil-structure interaction (SSI) and the soil nonlinearity effects are assumed beneficial and thus ignored. However, an accurate evaluation of the expected structural seismic response may improve engineering practice and reduce costs. The aim of this study is to assess the effects of SSI and soil nonlinearity on the structure's performance. First, the effect of the different sources of uncertainty on the SA and AF values is analyzed. Three important aspects are addressed: (1) the statistical model used to describe the variability of soil properties, (2) the ground motions used in the analyses, and (3) the soil constitutive model used. For this purpose, the results of several cyclic tests on alluvial soils are used to quantify the variability of the shear modulus degradation and damping evolution curves. Two sets of MRC are obtained and used in the consequent analyses. Then, several 1D finite element computations are performed with a coupled nonlinear model to represent soil behavior evaluating the effect of varying input motions and V_s profile variability. Finally, a typical reinforced structure is added to the model in 2D finite element computations to evaluate the SSI effect.

2. Site Conditions and modelled variability

The study case for this paper is the alluvial deposit zone. It is located in the center of the valley, along the Medellin River, and is characterized by broad sediment layers to depths up to 240 m [15]. Although classified as a homogeneous zone, these deposits consist of a wide variety of clays, silts, sands and coarse gravel distributed in pockets of horizontal and vertical spatial variability. In general, the vertical gradation is normal, from fine soils near the surface (silts, clays and sandy silts) to coarser sands and gravels at higher depth. However, some boreholes presented cross stratification with stiffer layers near the surface and even peat layers of 1 m thick at 3 m, below sandy layers. Often supported by clasts of fine to coarse grains, some rounded and varying shape coarse gravel and cobbles of 10-20 cm may be found throughout the finer layers [15].

According to 12 boreholes including SPT, down-holes and geophysical surveys, the average depth of the deposit, defined as the location where the V_s is above 760 m/s, is 28.5 m [16]. However, one borehole encountered an amphibolite layer of 5 m thick at 13 m while others presented alluvial layers up to 42 m. The average moist unit weight is almost constant throughout the deposit and equal to 17 kN/m³ with a coefficient of variation (COV) of 20%. The baseline V_s profile ranges from 225m/s near the surface to 823m/s at 42m. As previously noted the V_s average and standard deviation is given in the microzonation for each meter, presenting COV values fluctuating from 13% to 37%. The average V_{S30} is 419 m/s for the baseline profile. The corresponding T_{soil} is 0.26 s evaluated with the Haskell-Thomson analytical method for elastic conditions ([17], [18]). It is worth mentioning that as the motion intensity increases, more shear strains are developed in the deposit and more degradation of the V_s values in the profile is expected. Hence, the degraded profile will cause a shift of T_{soil} to longer periods and more damping will cause less amplification due to resonance.

2.1 Soil nonlinearity

Concerning the soil nonlinearity, data of seven cyclic triaxial and resonant column tests were taken into account to define MRCs and damping curves. The maximum shear modulus from resonant column and especially from triaxial tests $(G^{lab})_{max}$ is generally smaller to the *in-situ* measurements from down-hole or geophysics surveys $(G^{in-situ})_{max}$. According to a recompilation of triaxial test data, Tatsuoka et al. [19] estimated that $(G^{lab})_{max}$ may be up to half the $(G^{in-situ})_{max}$ when strain measurements are taken inside the triaxial test and up to ten times smaller if strain measurements are taken externally. Additional measurement errors in cyclic triaxial tests identified by Tatsuoka et al. [19] such as the piston deformation and friction, and the frictional forces near the sample contact with the caps, known as bedding, will result in an underestimation of the shear modulus and an overestimation of damping. To partially account for these errors, each set of test results was corrected following the equations presented by [20]:

$$\frac{G}{G_{max}} = \frac{1}{1 + \frac{\gamma}{\gamma_{0.5}}} \quad (1)$$

and

$$D = D_{min} + D_{max} \left[1 - \frac{G}{G_{max}} \right] \quad (2)$$

where the corrected G_{max} and $\gamma_{0.5}$ are obtained by linear regression of equation 1 for each set of data, and D_{min} and D_{max} are the minimum and maximum damping values from all available data. To combine all sets, all MRCs were normalized by the corrected G_{max} and the average and standard deviation are evaluated for $\gamma_{0.5}$. These values are 0.171 and 0.11626,



respectively, for the alluvial deposit. D_{min} is equal to 2.6% and D_{max} is 21.5%. Fig. 1 shows all the corrected data for the normalized MRCs and the damping curves. Additionally, the obtained average (μ) and plus and minus one standard deviation ($\mu \pm \sigma$) according to equations 1 and 2 are depicted with solid and dashed black lines, respectively. It is worth mentioning that some data points in both figures are below this region for higher shear strain levels, i.e. some data present more degradation and less damping at strain levels above 6×10^{-4} .

Moreover, the Darendeli [21] μ and $\mu \pm \sigma$ are also shown in solid and dashed red lines, respectively. These curves were evaluated for a confinement pressure of 150kPa (about the middle of the soil deposit) and a plasticity index of 15% according to average values found in this zone. The average Darendeli [21] MRC is very similar to the lower limit of the adjusted curves while the average damping curve presents considerable less damping for shear strains smaller than 0.02%, where the minimum damping is 1%. In addition, the variability presented by the adjusted curves is greater than that provided by Darendeli [21]. This variability measured as a COV of 68% for $\gamma_{0.5}$ is due to the combination of test data of different boreholes, evaluated at different confinement pressures, with different test systems and in different laboratories. Montoya-Noguera [22] developed a procedure to correct results from these two sets and Regnier et al. [23] used this procedure in the validation benchmark for seismic site response analysis. The corrected curves were in general softer, i.e. the modulus reduction was more important at intermediate strain levels, which will produce stronger effects of nonlinearity. Thus, similar to the Darendeli curves. In this study, to analyze the effect of the level of nonlinearity, two sets of curves will be used. The adjusted average curve will be called the stiff MRC while the average Darendeli curve is the soft MRC.

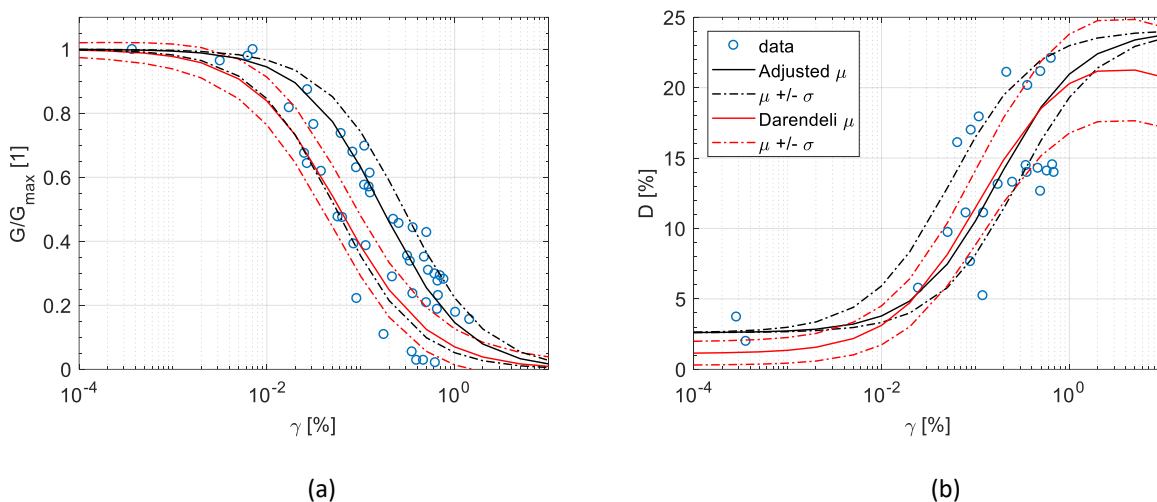


Fig. 1 a) Shear modulus reduction curves (MRC) and b) damping curves with respect to shear strain (data taken from [3])

2.2 Soil property variability

In geotechnical engineering, various studies have been performed to characterize uncertainties. Phoon and Kulhawy [5] provided typical average, COV and scale of fluctuation (or correlation distance) values for different strength properties. Concerning seismic hazard assessments, various studies considered uncertainty by randomized Monte Carlo simulations but often no correlation (statistical independence) or complete correlation is assumed between layers and soil parameters. Toro [24] developed a model for the interlayer correlation from an analysis of over 500 Vs profiles. Rathje et al. (2010) evaluated the effect of different values of interlayer correlation. They showed that less correlation of the Vs values between layers resulted in a decrease in the median values of SA and AFs and almost no effect on the standard deviation. These results are disquieting as they show that the expected response may be underestimated when no correlation is included. The procedure proposed by Yamin et al. [3] and used to evaluate the AFs for the different zones in AMVA, considered the uncertainty in the bedrock depth, the soil layer thicknesses, the shear-wave velocity profile, the unit weight and the MRC curves simultaneously. Normal and lognormal distributions were used, each of these variables was assumed independent and no spatial correlation was used.

In this paper, randomized Vs profiles generated for Monte Carlo simulations are based on the baseline Vs profile defined by the average values provided each meter. Karhunen-Loève (KL) expansion is used to simulate the random field samples (RFSs) according to the methodology detailed in Montoya et al. [25]. To model shear wave velocity variability a lognormal distribution is used. The random field is assumed stationary with an average coefficient of variation COV_{Vs}



about 20% and the modified exponential covariance function [26] with a correlation length of 20m, which according to Rathje et al. [10] provides control to the amount of V_s inversions and avoid high impedance contrasts and too soft soil profiles. A Q-Q probability plot between the marginal cumulative distribution function (CDF) obtained from the generated 200 RFSs for a lognormal distribution and the theoretical CDF is shown in Fig. 2a. The generated RFSs match reasonably well the theoretical distribution considering the limited number of finite elements used and the computational cost involved in increasing the number of RFSs. Fig. 2b shows all the RFSs generated as the V_s profiles for the site response analysis. It is worth noting that the baseline V_s profile, shown as a black line, includes inversions at depths of 35m.

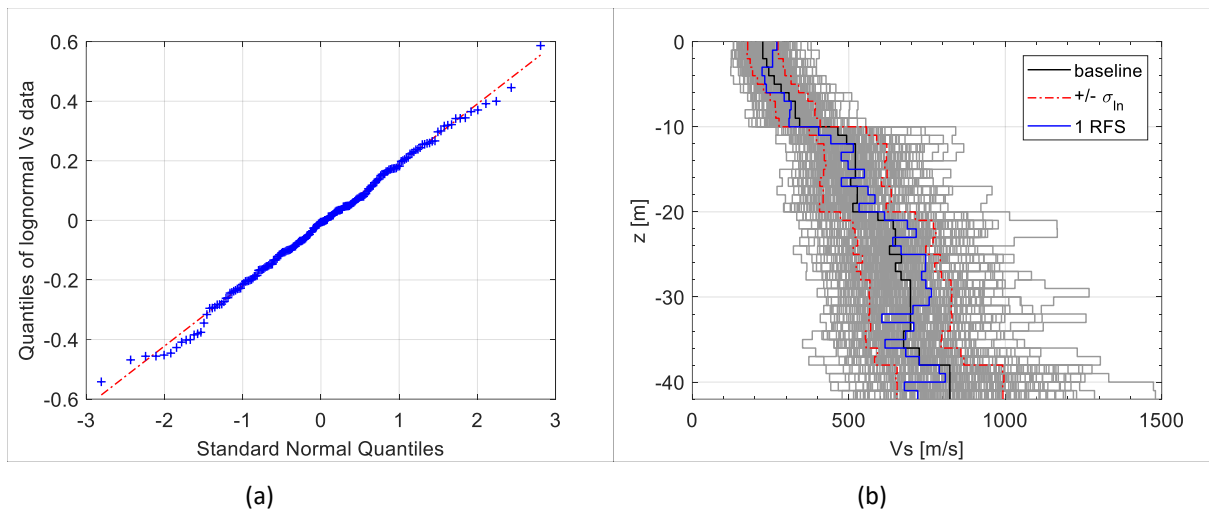


Fig. 2 Random field samples: a) QQ plot with respect to theoretical CDF and b) resulting V_s profiles

According to this randomization of the V_s profile, the effect on V_{s30} and T_{soil} was investigated. Again, the T_{soil} values are obtained by the Haskell-Thomson analytical method for the initial elastic behavior. Fig. 3 presents the resulting histograms. Also in the figures, a vertical black line depicts the baseline value and the red curve the obtained lognormal distribution. The mean values obtained for this distribution are very close to the baseline values: V_{s30} is 402 m/s with respect to the initial 419 m/s, and T_{soil} is 0.27 s with respect to an initial value of 0.26 s. The resultant COV for T_{soil} is 12.7%. According to the obtained V_{s30} values, the site is classified as C and D according to NEHRP and NSR-10. The average V_{s30} value presented by Prada et al. [16] was 376m/s and the average T_{soil} was 0.28 s with a COV value of 46%, assuming independent and uncorrelated variables. This higher variability results in profiles with V_{s30} as low as 150m/s and T_{soil} above 0.7s. In contrast, this study includes only T_{soils} below 0.4s and V_{s30} above 250 m/s.

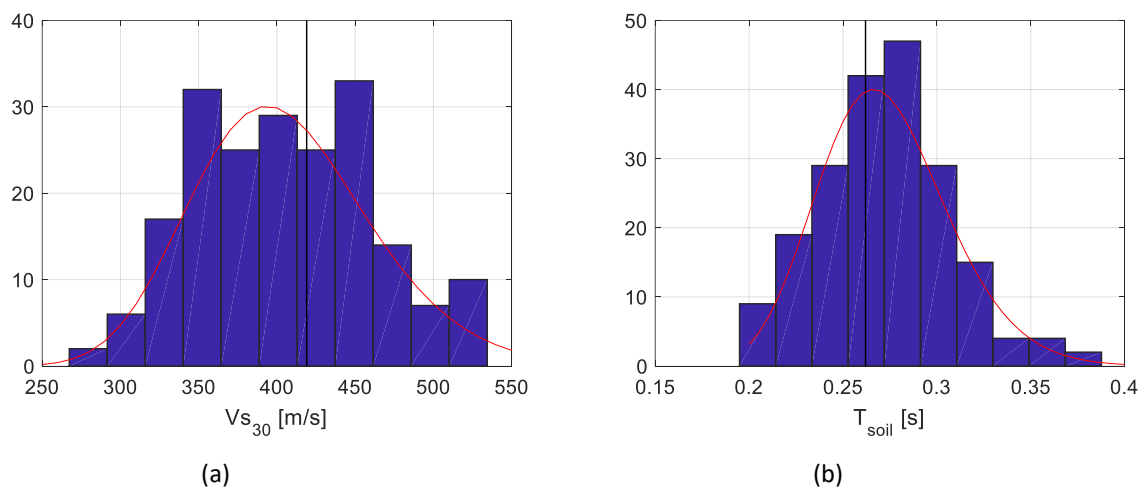


Fig. 3 Histograms for the upper 30 m average shear wave velocity and for the fundamental soil period

3. Numerical model

3.1 Input earthquake motions



The input motions used correspond to unscaled real earthquake signals recorded in dense soil stations from near-to-source earthquakes of moment magnitudes (M_w) between 5.6 and 6.7. These signals are appropriate for the numerical model hypothesis of outcropping rock and deformable bedrock. The signals were obtained from the Pacific Earthquake Engineering Research Center (PEER) database. The selected motions identification and some intensity measures (IM) are shown in Table 1. Both horizontal components were used and the IM values correspond to the maximum for each station. The order in the table correspond to the ascending values of peak horizontal acceleration (PHA), however, the increase in peak horizontal velocity (PHV), Arias intensity (I_A) and significant duration (D_{5-95}) do not coincide with this increase in PHA. Fig. 4 shows the acceleration response spectra of the input motions with a 5% structural damping. Note that in general, the energy is shifted to longer periods as the PHA increases, however; a large variation is present in the spectral amplitudes at different periods.

Table 1 – Input motions' identification and some intensity measures

ID	Earthquake	Year	RSN*	M_w	R_{JB}^+ [km]	V_{S30} [m/s]	PHA [g]	PHV [cm/s]	I_A [cm/s]	D_{5-95} [s]
1	L'Aquila (AS1)	2009	4513	5.6	5.07	717	0.09	6.98	6.9	13.4
2	Whittier Narrows-01	1987	680	5.99	6.78	969.07	0.11	10.32	8.7	6.2
3	Morgan Hill	1984	454	6.19	14.83	729.65	0.11	3.64	5.7	8.6
4	Coyote Lake	1979	146	5.74	10.21	1428.1	0.12	10.81	7.9	6.8
5	Sierra Madre	1991	1649	5.61	37.63	996.43	0.12	2.98	3.9	4.4
6	Northridge-01	1994	1091	6.69	23.1	996.43	0.15	18.38	37.4	8.3
7	San Fernando	1971	80	6.61	21.5	969.07	0.20	12.84	34.3	14.1
8	Tottori_Japan	2000	3954	6.61	15.58	967.27	0.23	21.46	48.4	12.8
9	Parkfield-02 CA	2004	4083	6	4.66	906.96	0.24	14.61	18.8	8.8
10	Friuli_Italy-01	1976	125	6.5	14.97	505.23	0.36	30.52	120.2	4.9

*Record sequence number, ⁺Joyner-Boore source-to-site distance.

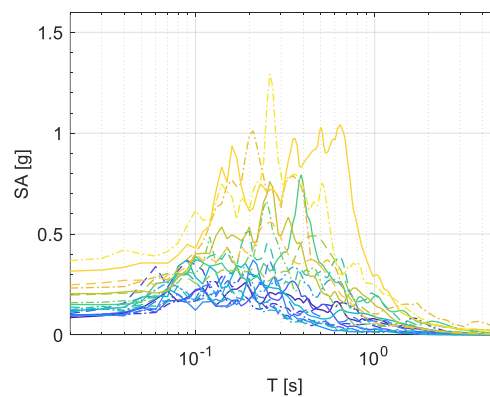


Fig. 4 Pseudo Spectral Acceleration of input motions with 5% damping

3.2 Numerical model

Finite element computations with plain-strain assumption were performed in GEFDyn [27]. This program allows the modeling of both soil and structural nonlinear behavior for static and dynamic loading. The saturated soil was modelled using quadrilateral isoparametric elements with eight nodes for both soil displacements and fluid pressures. A 2D model is used as the soil is assumed horizontally homogeneous and on vertically propagating plane S waves are considered. The 2D model was 50 m wide and 42 m deep, according to the maximum depth characterized by the V_s and moist unit weight profiles. Numerical damping of 1% is added in the Newmark integration scheme to assure unconditional stability with optimal high-frequency dissipation and minimum low-frequency impact [22]. At the base of the model, a deformable



unbounded elastic bedrock is simulated with paraxial elements [28]. The input motions are introduced at the base of the model after deconvolution as these are assumed to be at outcropping bedrock conditions.

The soil constitutive model used is the ECP model [27], which is able to simulate the fully elastoplastic behavior. The ECP model depends on effective stresses, follows the critical state concept, and uses a Coulomb-type failure criterion. This model is able to simulate the behavior of soils for a large range of deformations due to its decomposition into pseudo-elastic, hysteretic, and mobilized domains. The soil model parameters are determined with the procedure defined in Lopez-Caballero and Modaressi-Farahmand-Razavi [12]. The engineering bedrock representing a half-space medium is modeled with an isotropic linear elastic behavior. The structure used is a typical reinforced concrete building with shallow rigid foundation. A two-story structure is modeled as a large-scale one-span frame with plastic hinge beam-column elements that account for axial force and bending moment interaction. This model was proposed and developed by Saez et al. ([29]).

3. Results and analysis

As shown previously, including the variability of various sources in seismic hazard assessment is highly complex, especially when nonlinearity is taken into account. Thus, separate analyses will be presented concerning the different sources of uncertainty.

3.1 Effect of input motion variability on the computed response

The use of recorded input motions involves large variations at different periods as shown previously in Fig. 4. Thus, the amplification factor (AF) evaluated as the ratio between the obtained surface spectra and the spectra at the outcropping bedrock presents large variability with respect to the input motion used. The AF results for the twenty input motions are shown in Fig. 5 for the baseline V_s profile and the two modulus reduction curves (MRC). The same color code of input motion PHA values shown in Fig. 4 is used in this figure. The results for the input motions used and the deposit with stiff MRC (see Fig. 5a) present amplification at almost all periods with the largest amplifications of up to eight occurring around periods between 0.3 and 1s. However, the effects of nonlinearity are evident in the decrease of this amplification at shorter periods for input motions of higher PHA and a shift of the energy towards longer periods.

Concerning the results of the deposit with soft MRC (see Fig. 5b), a deamplification of almost all accelerations is evidenced for periods below 0.2s. Additionally, the shift to longer periods is more pronounced. For example, for the input motion of highest PHA value (PHA = 0.36g), accelerations are amplified only for periods above 1s. The level of degradation of the shear modulus throughout the profile results in longer resonant periods ranging from 0.5s to almost 1s. For the results shown it is evident that combining both input motion and MRC variability will produce AF values closer to unity and no clear evidence of the shift to higher periods.

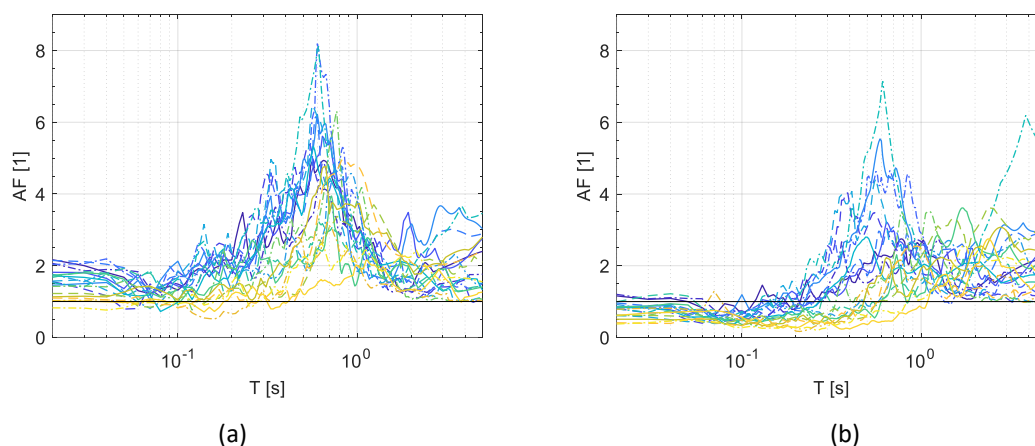


Fig. 5 Amplification factors for the baseline V_s profile and a) the stiff MRC and b) the soft MRC

3.2 Effect of the V_s profile variability

Monte Carlo simulations of the nonlinear site response were performed using the 2 sets of MRC and the 200 V_s profiles shown in Figure 2b. Three input motions were used: the one with the smallest PHA value (EQ1, L'Aquila earthquake with PHA= 0.09g), an intermediate PHA value (EQ5, Sierra Madre earthquake with PHA = 0.12g, and the one with the



highest PHA value (EQ10, Friuli earthquake with PHA = 0.26g). This change in PHA value will induce more nonlinearity in the response.

The response spectra of acceleration (SA) at the surface of the deposit is shown in Fig. 6 for all the Vs profiles using the stiff and the soft modulus reduction curves (MRC) and the strongest motion. The color code is defined by the elastic resonant period of the soil (T_{soil}). In addition, the SA curve of the input motion is shown in red line. It is evident that the effect of the MRC in the response is important but highly complex. When the MRC is stiffer (see Fig. 6a and 6c), less nonlinearity is expected. Hence, the PHA at surface – i.e. the SA for the shortest period - is higher than at the outcropping rock and, generally, the accelerations at all periods are amplified. However, due to the strong intensity of the input motion, even if the modulus reduction is not important for intermediate strains, there is an evidence of a shift to longer periods. This is evident in that the maximum amplification is presented for periods longer than the T_{soil} values, although there is still an amplification around these periods. In contrast, when the modulus reduction starts at lower shear strains (see Fig. 6b and 6d), a strong deamplification is evident at shorter periods while a weak amplification is presented for periods above 0.35s.

Concerning the effect of the T_{soil} value on the response, it is shown that for the stiff MRC, the largest amplification at 0.8s and the AF values at longer periods are related to the highest T_{soil} value. However, for shorter periods the relation between T_{soil} and AF is not evident. In contrast, for the soft MRC results, the T_{soil} value does not have a clear relation with the AF values.

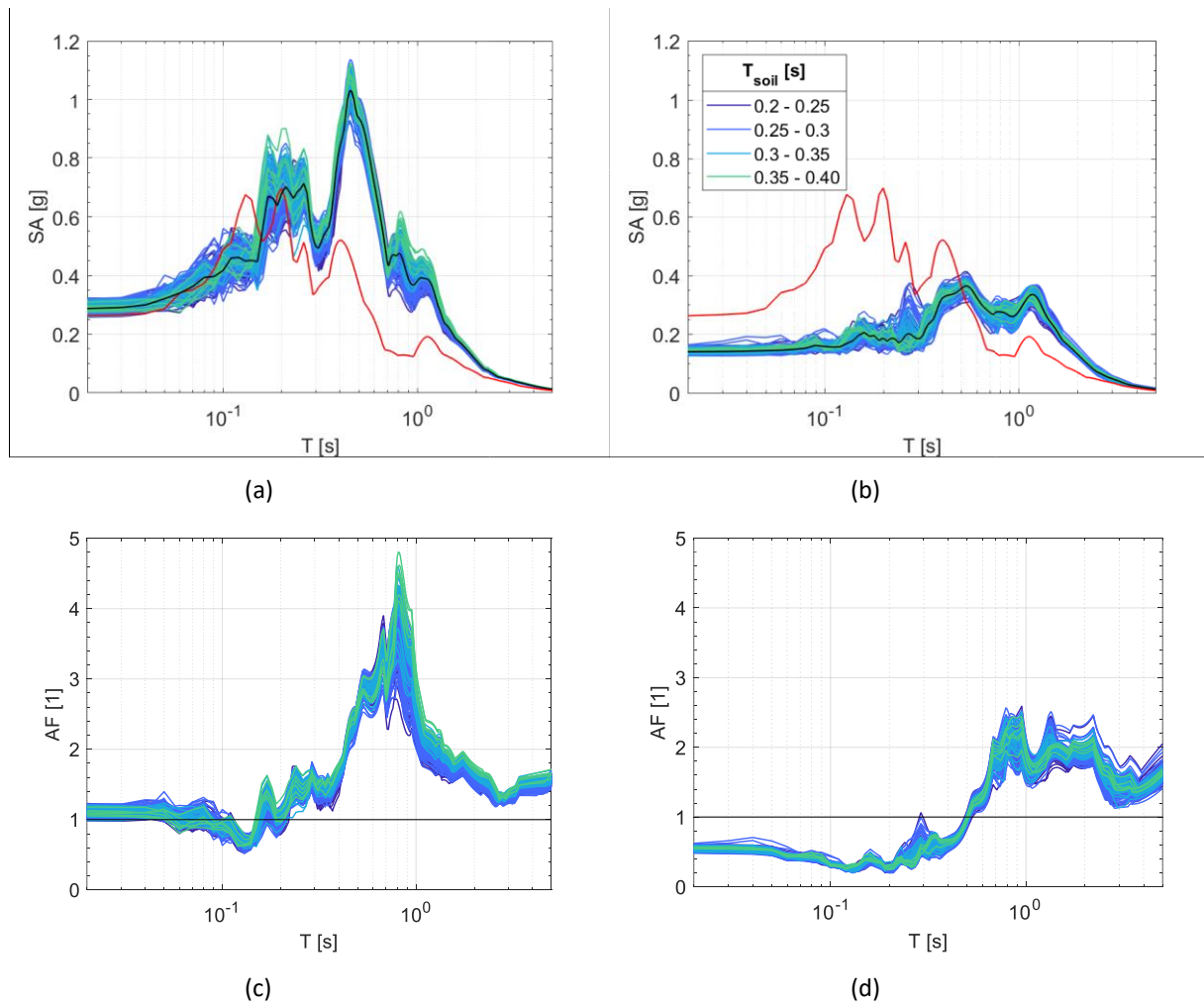


Fig. 6 SA at surface and AF for stiff MRC with EQ10 (a and c) and soft MRC (b and d)

The envelope of all the AF results is shown in Fig. 7 for each set of MRC and input motion used. For the weakest input motion (see Fig. 7a), both deposits present an amplification of the PHA value at surface, but with the stiffer MRC the maximum amplification is about twice that of the softer MRC and is presented at a shorter period –i.e. maximum AF of about 6 at $T = 0.55s$, and a value of 3.2 at $T = 0.8s$. In general, nonlinear effects are not considered for weak motions;



however, these results show that the level of degradation of the shear modulus may affect the response even for input motions with PHA values of 0.09g.

Concerning the strongest input motion (see Fig. 7c), the PHA at surface is amplified for almost all Vs profiles when the stiff MRC is used but it is deamplified for all cases when the soft MRC is used. For this input motion, the maximum amplification of about five is clearly shown for a period of 0.8s when the stiff MRC is used but with the soft MRC no clear resonant period is shown and a maximum amplification of about 2.5 is presented for periods ranging from 0.8s to almost 2.5s. Concerning the resultant variability in AF, the weakest motion causes more variability in the response while it is strongly reduced when the strongest input motion is used. However, combining the AF results for both sets of MRC will result in high variability at periods below 1s and smaller variability for longer periods as both regions overlap. In addition, an average of AF results will counteract the amplification of stiff MRC with the deamplification of soft MRC for shorter periods, especially for periods below the elastic fundamental period of the soil. This average may also fail to identify the shift to longer periods particularly important for strong input motions.

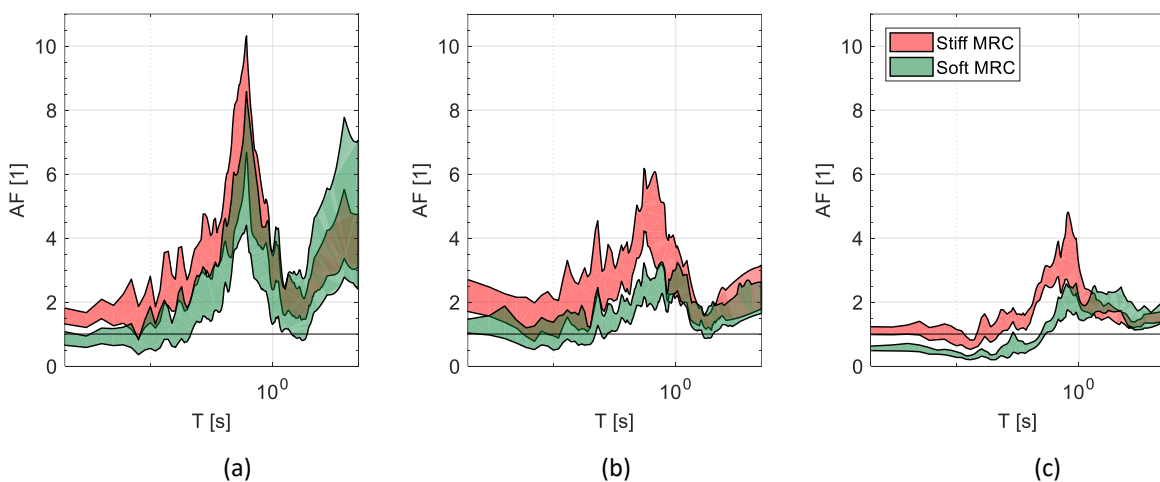


Fig. 7 Amplification factors with Vs profile variability for input motions a) EQ1, b) EQ5 and b) EQ10.

3.3 Comparison of the effect of the input motion, MRC and Vs profile variability

The variability of AF results about the median values due to the different sources of variability is evaluated. This variability is quantified by the standard deviation (σ) and the coefficient of variation (COV) for the logarithmic SA and AF values. Results are shown in Fig. 8. The σ AF values are generally smaller than the σ SA values because AF is normalized by the response spectra of the input motion, which reduces the influence of record-to-record variability. In Fig. 8a, the variability of the input motions SA shown in Fig. 4 is shown in blue, and the SA variability of the corresponding surface response for each input motion with stiff MRC and soft MRC are shown in red and green lines, respectively. The $\sigma \ln(\text{SA})$ values are larger at the outcropping rock and lower for the soft MRC. In general, there is less variability at shorter periods but for the stiff MRC and the soft MRC results, the variability change between shorter and longer periods is evident for higher values. Results of the variability for each earthquake input motion and each MRC curve are also shown in dotted lines. The $\sigma \ln(\text{AF})$ values evidence the increase in variability due to the resonant period and its shift. For instance, the largest standard deviation is presented at 0.5s, however the respective COV value is not large as this value corresponds to the period at resonance. With regard to the 20% of COV for the Vs profile, the average COV AF is about 6% and the largest value presented is 20% for individual cases of input motion and MRC curve. Hence, the nonlinearity expressed by the modulus reduction causes that the variability of the AF results is lower than the variability in the initial Vs profile. However, when all sources of variability are combined (black line), that is when both input motions, both MRC curves and the Vs randomness is included, the resultant $\sigma \ln(\text{AF})$ and COV AF are almost as large as the variability due to all input motions used.

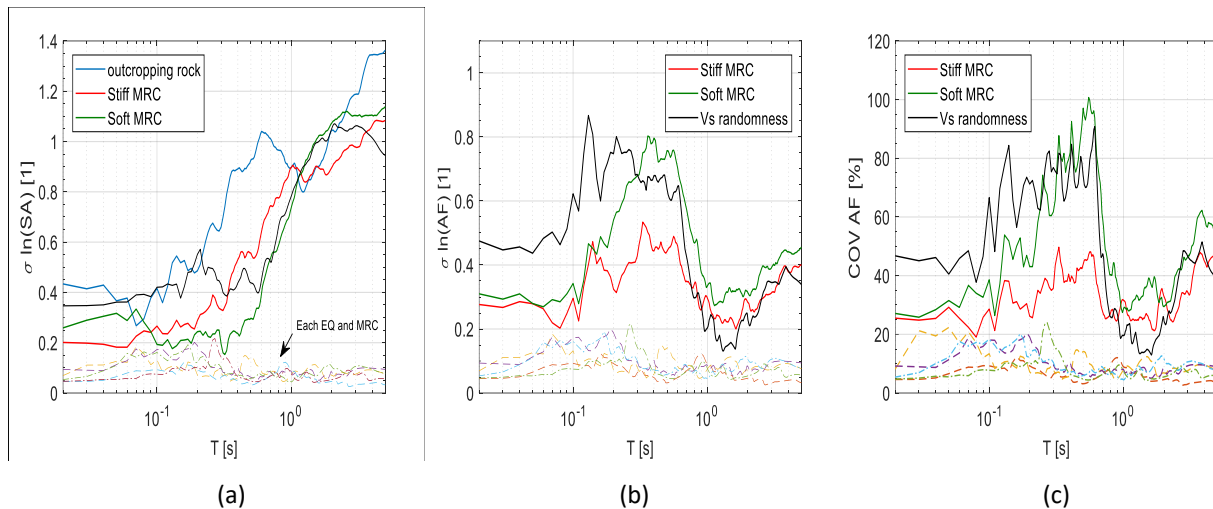


Fig. 8 Variability in the response: logarithmic standard deviation of a) SA and of b) AF, and c) COV of AF

3.4 Effect of the soil-structure interaction

A pseudo-static analysis of the soil-structure model is performed with a scaled motion at a very low amplitude –i.e. PHA = 1E-5g, to ensure quasi-elastic behavior of both soil and structure. The transfer function (TF) is evaluated as the ratio between the Fast Fourier Transforms of the acceleration time history at different locations of the model. TF is evaluated for four couples to identify the differences between the free field (FF), the base of the bedrock (bd), and the base and top of the structure. Results, presented in Fig. 9, show that the structure has an effect on the soil as seen in base/bd (green) compared to FF/bd (red). Simultaneously, the soil has an effect on the structure as seen in top/FF (blue) compared to top/base. In this case, while the fundamental resonant frequency of the structure with fixed base is about 7Hz, the SSI resonant frequency is about 5.5Hz.

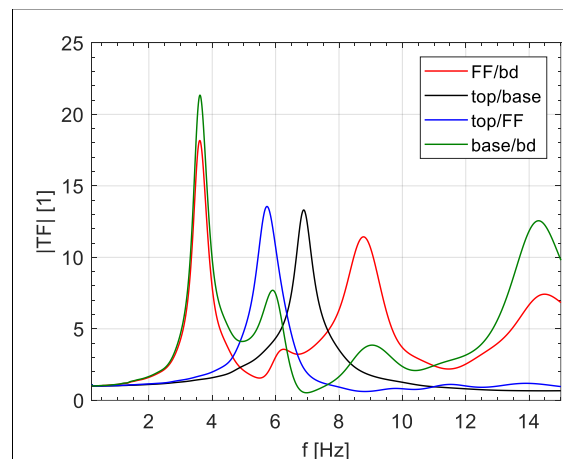


Fig. 9 Transfer function at different locations of the soil-structure model

The effect of the SSI on the response was analyzed for six input motions, the two MRCs and the concrete-frame structure presented previously. The results of the peak ground acceleration (PGA) at the free field surface (i.e. with the 1D model) with respect to the PHA value at the outcropping rock are shown in Fig. 10a. The input motions used in the soil-structure model are shown with filled symbols. These show an amplification at surface when the stiff MRC is used, and a deamplification when the soft MRC is used. In average, the PGA with stiff MRC is twice the PGA with soft MRC and this ratio appears not to be influenced by the PHA value. Fig. 10b and 10c show the results of the inter story drift (ISD) and the relative settlement of the structure with respect to free field (u_z). Concerning ISD, the structure on stiff MRC will present higher values and the ratio with the soft MRC appears to increase with the PHA level from a 13% increase to more than twice. In contrast, the estimated u_z is in some cases higher when the soft MRC is used. Furthermore, the relation of u_z for the stiff and soft MRC appears not to be related with the PHA level. Thus, the relative settlement of a structure appears to depend on other intensity measures as well, for example, the Arias intensity or the PHV value of the input motion.

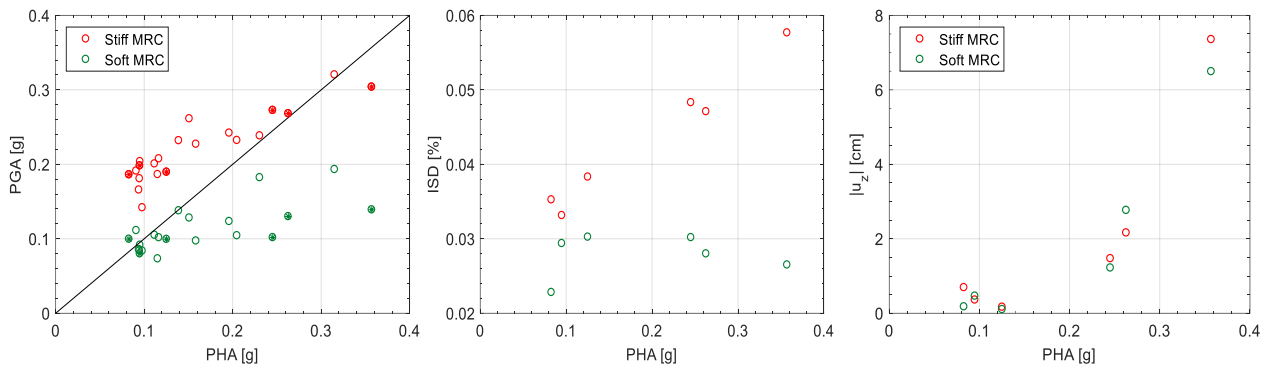


Fig. 10 a) PGA vs PHA for all input motions, b) inter-story drift and c) relative settlement for selected motions

4. Conclusions

The most recent microzonation study in AMVA included site effects by performing multiple Monte Carlo simulations of 1D linear-equivalent analyses including simultaneously different sources of uncertainty such as different input motions, variability in V_s profiles and variability in MRC. This paper focused in understanding the effect of each source of uncertainty when a fully nonlinear soil model is used. For the alluvial site, the results show that the amplification factors are significantly affected by the input motion used, and not only its PHA value. The reason is that more nonlinearity affects differently the short period deamplification from the long period amplification. In this study, the MRC variability affected the most the response, especially in intermediate periods around the elastic resonant period of the soil. In contrast, the V_s variability affected only slightly the AF values.

The combined effect of variability of input motion and MRC, and soil-structure interaction is significant when strong nonlinearity is expected. Peak acceleration differences observed between the surface and the outcropping rock at 1D models when soft and stiff MRC are used, appear to be independent of the PHA value. However, the response at the top of the structure for the site and motions tested with stiff MRC presented higher structural demand (i.e. higher ISD values) because the strain level at the soil deposit is lower and no significant degradation of the V_s profile nor high soil damping is present. However, when soft MRC is used, the response at the top of the structure differs greatly and appears to be independent of the PHA level. The effects of using different modulus reduction curves are not the same for ISD values as on the values of the relative settlement.

Hence, the results highlight the importance of first, accurately assessing, and then, modeling the nonlinear behavior of the soil deposit to evaluate SSI and the expected response of the system. This study evaluated only the response of one of the geological zones and one typical structure; however, the complex effects of soil nonlinearity on the soil-structure response should be evaluated for different structures. This systematic investigation should provide insights into the dominant sources of variability depending on the soil, the structure, and the input motion used.

5. References

- [1] V. Silva *et al.*, “Development of a global seismic risk model,” *Earthq. Spectra*, no. February, p. 875529301989995, 2020.
- [2] A. B. Acevedo, J. D. Jaramillo, C. Yepes, V. Silva, F. A. Osorio, and M. Villar, “Evaluation of the seismic risk of the unreinforced masonry building stock in Antioquia, Colombia,” *Nat. Hazards*, vol. 86, pp. 31–54, 2017.
- [3] L. E. Yamin *et al.*, “Practical seismic microzonation in complex geological environments,” *Soil Dyn. Earthq. Eng.*, vol. 114, no. May, pp. 480–494, 2018.
- [4] E. H. Vanmarcke, “Probabilistic Modeling of Soil Profiles,” *J. Geotech. Eng. Div.*, vol. 103, no. 11, pp. 1227–1246, 1977.
- [5] K.-K. K.-K. Phoon and F. H. Kulhawy, “Characterization of geotechnical variability,” *Can. Geotech. J.*, vol. 36, no. 4, pp. 612–624, 1999.
- [6] G. A. Fenton and D. V. Griffiths, *Risk Assessment in Geotechnical Engineering*. 2008.
- [7] Z. Cao and Y. Wang, “Bayesian Model Comparison and Characterization of Undrained Shear Strength,” *J. Geotech. Geoenvironmental Eng.*, vol. 140, no. 6, 2014.



- [8] Y. Wang and A. E. Aladejare, "Evaluating variability and uncertainty of Geological Strength Index at a specific site," *Rock Mech. Rock Eng.*, vol. 49, no. 9, pp. 3559–3573, 2016.
- [9] T. Zhao, S. Montoya-Noguera, K.-K. K.-K. Phoon, and Y. Wang, "Interpolating spatially varying soil property values from sparse data for facilitating characteristic value selection," *Can. Geotech. J.*, vol. 55, no. 2, pp. 171–181, 2018.
- [10] E. M. Rathje, A. R. Kottke, and W. L. Trent, "Influence of Input Motion and Site Property Variabilities on Seismic Site Response Analysis," *J. Geotech. Geoenvironmental Eng.*, vol. 136, no. 4, pp. 607–619, 2010.
- [11] W. Li and D. Assimaki, "Site- and motion-dependent parametric uncertainty of site-response analyses in earthquake simulations," *Bull. Seismol. Soc. Am.*, vol. 100, no. 3, pp. 954–968, 2010.
- [12] F. Lopez-Caballero and A. Modaressi-farahmand-razavi, "Assessment of variability and uncertainties effects on the seismic response of a liquefiable soil profile," *Soil Dyn. Earthq. Eng.*, vol. 30, no. 7, pp. 600–613, Jul. 2010.
- [13] NEHRP, *RECOMMENDED PROVISIONS FOR SEISMIC REGULATIONS FOR NEW BUILDINGS AND OTHER STRUCTURES (FEMA 450)*, no. Fema 450. Washington, D.C, 2003.
- [14] Ministerio Ambiente Vivienda y Desarrollo Territorial, "NSR-10 Requisitos generales de diseño y construcción sismo resistente," *Nsr-10*, vol. Titulo A, p. 53, 2010.
- [15] D. A. Rendón, "Tectonic and sedimentary evolution of the upper Aburrá Valley, northern Colombian Andes," Shimane University, Japan, 2003.
- [16] E. Prada, L. E. Yamin, and R. R. Garcia, "Incertidumbre en la respuesta dinámica unidimensional de depósitos de suelos para efectos de microzonificación sísmica One-dimensional dynamic response uncertainty of soil deposits for seismic microzonation purposes," no. June, 2017.
- [17] W. T. Thomson, "Transmission of elastic waves through a stratified solid medium," *J. Appl. Phys.*, vol. 21, no. 2, pp. 89–93, 1950.
- [18] N. A. Haskell, "Dispersion Waves Abstract," *Bull. Seismol. Soc. Am.*, vol. 43, no. 1, pp. 17–34, 1953.
- [19] F. Tatsuoka, D. C. F. Lo Presti, and Y. Kohata, "Deformation characteristics of soils and soft rocks under monotonic and cyclic loads and their relationship," in *Third International Conference on Recent Advances in Geotechnical Earthquake Engineering and Soil Dynamics*, 1995.
- [20] K. Ishihara, "Liquefaction and flow failure during earthquakes," *Géotechnique*, vol. 43, no. 3, pp. 351–451, Sep. 1993.
- [21] M. B. Darendeli, "Development of a new family of normalized modulus reduction and material damping curves," University of Texas at Austin, 2001.
- [22] S. M. Noguera, "Assessment and mitigation of liquefaction seismic risk : numerical modeling of their effects on SSI," Université Paris-Saclay, 2016.
- [23] J. Régner *et al.*, "Prenolin: International benchmark on 1D nonlinear: Site-response analysis—validation phase exercise," *Bull. Seismol. Soc. Am.*, vol. 108, no. 2, pp. 876–900, 2018.
- [24] G. R. Toro, "Probabilistic models of site velocity profiles for generic and site-specific ground-motion amplification studies," Upton, N.Y, 1995.
- [25] S. Montoya-Noguera, T. Zhao, Y. Hu, Y. Wang, and K.-K. K.-K. Phoon, "Simulation of non-stationary non-Gaussian random fields from sparse measurements using Bayesian compressive sampling and Karhunen-Loève expansion," *Struct. Saf.*, vol. 79, no. March, pp. 66–79, 2019.
- [26] P. D. Spanos, F. Asce, M. Beer, M. Asce, and J. Red-horse, "Karhunen – Loève Expansion of Stochastic Processes with a Modified Exponential Covariance Kernel," no. July, pp. 773–779, 2007.
- [27] D. Aubry and H. Modaressi, "un modèle de sols saturés en dynamique non linéaire (a model for the non linear dynamic analysis of saturated soils) un modèle de sols saturés en dynaOlique non linéaire a model for the non linear dynamic analysis of saturated soils," *Rev. Fr. Géotechnique*, vol. 46, pp. 43–75, 1989.
- [28] H. Modaressi and I. Benzenati, "Paraxial approximation for poroelastic media," *Soil Dyn. Earthq. Eng.*, vol. 13, no. 1, pp. 117–129, 1994.
- [29] E. Saez, F. Lopez-Caballero, and A. Modaressi-farahmand-razavi, "Effects of non-linear soil behaviour on the seismic performance evaluation of structures," *Riv. Ital. DI Geotec.*, vol. 2, pp. 63–76, 2008.